The Kinetics of the Radiative and Nonradiative Processes in Nanocrystalline ZnO Particles upon Photoexcitation

Addy van Dijken,*,† Eric A. Meulenkamp,‡ Daniël Vanmaekelbergh,† and Andries Meijerink†

Debye Institute, Utrecht University, P.O. Box 80.000, 3508 TA Utrecht, The Netherlands, and Philips Research Laboratories Eindhoven, WA 13, Prof. Holstlaan 4, 5656 AA Eindhoven, The Netherlands

Received: September 17, 1999; In Final Form: December 4, 1999

This report presents the results of steady-state and time-resolved luminescence measurements performed on suspensions of nanocrystalline ZnO particles of different sizes and at different temperatures. In all cases two emission bands are observed. One is an exciton emission band and the second an intense and broad visible emission band, shifted by approximately 1.5 eV with respect to the absorption onset. As the size of the particles increases, the intensity of the visible emission decreases while that of the exciton emission increases. As the temperature decreases, the relative intensity of the exciton emission increases. In accordance with the results presented in a previous paper, we assume that the visible emission is due to a transition of an electron from a level close to the conduction band edge to a deeply trapped hole in the bulk ($V_O^{\bullet\bullet}$) of the ZnO particle. The temperature dependence and size dependence of the ratio of the visible to exciton luminescence and the kinetics are explained by a model in which the photogenerated hole is transferred from the valence band to a $V_O^{\bullet}$ level in the bulk of the particle in a two-step process. The first step of this process is an efficient surface trapping, probably at an O^{2-} site.

1. Introduction

ZnO has been known as a luminescent material for a century, and some fifty years ago it was discovered that firing ZnO powder in a reducing atmosphere gives a particularly efficient blue-green luminescent material. This is usually represented as ZnO:Zn because of the loss of oxygen during the reducing treatment.[1] This material has a high efficiency as a low-voltage phosphor and the material has been used in vacuum fluorescent displays (VFDs) and field emission displays (FEDs). Especially the latter application has become important recently, since FEDs are one of the promising candidates for flat panel displays.[2] Inspired by the application of ZnO, numerous studies have appeared on the nature of the visible luminescence from ZnO. Despite all this research, the mechanism behind the visible luminescence has been very difficult to establish, as is clear from a statement in the 1999 edition of the Phosphor Handbook: *"The origin of the luminescence center and the luminescence mechanism of ZnO:Zn phosphors are barely understood."*[2]

Much of the research on the luminescence of ZnO is performed on single crystalline powders (μm size) or single crystals. Two emission bands are usually found. A relatively weak and narrow UV emission band is observed around 380 nm (3.25 eV), just below the onset of absorption. A much stronger and broader emission band is situated in the green part of the visible spectrum, with a maximum between 500 and 530 nm (2.35−2.50 eV). The UV emission band is due to the radiative annihilation of excitons and can still be observed at temperatures far above room temperature due to the relatively high exciton binding energy of 59 meV.[3] The lifetime of this exciton emission is very short, on the order of several tens to hundreds of picoseconds.[4]

As mentioned before, the nature of the visible emission has been the subject of much research. At first, this emission was thought to be associated with divalent copper impurities,[5] but later intrinsic defects such as interstitial zinc ions[6] or oxygen vacancies[7] were assumed to be the recombination centers. Alternative explanations involved zinc vacancies,[8] chemisorbed oxygen,[9] and sulfur impurities.[10] During the past years, oxygen vacancies have been assumed to be the most likely candidates for the recombination centers involved in the visible luminescence of ZnO.[11−13] In contrast to the exciton emission, the lifetime of the visible emission is much longer, viz. in the μs range.[11]

Studies on the nature of defect centers which are involved in the visible emission often use treatment of macrocrystalline ZnO in a reducing or oxidizing atmosphere. In this way, the number of oxygen vacancies or other defects can be varied, and this is then related to changes in the luminescence intensity. A problem is that the intensity of the luminescence is influenced by the width of the depletion layer, which is also strongly dependent on defect concentrations. This makes it difficult to derive conclusions on the origin of the visible luminescence from the observed changes in the luminescence intensity and defect concentrations.[13−15] On the other hand, this indicates that the visible emission originates from the bulk of the material. In this study, nanocrystalline ZnO particles are used, which has two main advantages. First, there is no band bending in the particle as the particles are much smaller than the width of the depletion layer. Changes in luminescence intensity due to depletion layer effects are therefore absent. Second, the mean particle size can be varied and its influence on the emission properties can be studied since the electronic structure of ZnO

† Utrecht University.
‡ Philips Research Laboratories Eindhoven.

10.1021/jp993327z CCC: $19.00
Published on Web 02/03/2000

is size dependent when the particles are in the quantum size regime ($R \lesssim 20$ Å[16]). Studies on the variation of the energetic position of the maximum of both the visible and UV emission band as a function of particle size have provided additional information on the nature of the visible luminescence center. We have shown in a previous publication that the visible emission from nanocrystalline ZnO particles is due to a transition of a photogenerated electron from the conduction band to a deeply trapped hole.[17] The fact that the emission properties of macrocrystalline ZnO and nanocrystalline ZnO particles are very similar leads to the conclusion that the origin of the visible emission is the same for all forms of ZnO. However, the kinetics involved in the emission processes can be very different for nanocrystalline ZnO particles and for macrocrystalline ZnO. This will be the main topic of the present paper.

Although research on quantum size effects in small ZnO particles has been performed before,[18,19] the influence of temperature and size on both the steady-state and time-resolved luminescence was not studied. For this study, both steady-state and time-resolved emission measurements were performed on suspensions of nanocrystalline ZnO particles as a function of particle size and temperature. The temperature dependence of the emission intensities and emission lifetimes was studied by freezing the suspensions to liquid helium temperature. Based on the observations, the kinetics involved in the luminescence of nanocrystalline ZnO and the nature of the trap involved in the visible emission are discussed. A model is proposed for the competition between ultraviolet exciton recombination, trap recombination giving rise to visible luminescence, and non-radiative recombination in fair agreement with the results from the steady-state and time-resolved measurements.

2. Experimental Section

2.1. Sample Preparation. Suspensions of nanocrystalline ZnO particles can be prepared in nonaqueous solvents such as ethanol or 2-propanol. For the preparation in 2-propanol,[18] 25 mL of a 0.02 M NaOH solution was slowly added while stirring to 225 mL of a 0.001 M $Zn(CH_3COO)_2 \cdot 2H_2O$ solution, after both solutions were first cooled to 0 °C. The preparation in ethanol is very similar.[20,21] In this case, 50 mL of a 0.14 M $LiOH \cdot H_2O$ solution (prepared using an ultrasonic bath) was added to 50 mL of a 0.1 M $Zn(CH_3COO)_2 \cdot 2H_2O$ solution. Again, both solutions were first cooled to 0 °C before the hydroxide solution was added slowly to the zinc solution while stirring. The preparation in ethanol yields a suspension with a particle concentration about 2 orders of magnitude higher than the 2-propanol preparation. The kinetics of the particle growth is not the same for both preparations, but in both cases a rapid formation of extremely small ZnO particles is followed by a relatively slow growth of the particles.[21,22] The rate of particle growth depends strongly on the temperature. When the suspension is aged at room temperature, it takes several days for the particles to attain their final size. In ethanol, the rate of growth of ZnO particles is somewhat slower than in 2-propanol. TEM measurements have shown that the mean particle diameter of the fully grown particles is about 60 Å.[23] This corresponds to particles that contain approximately 5000 molecular ZnO units.

Directly after mixing the two starting solutions, the resulting reaction mixture is stored at room temperature. At regular intervals, a sample is taken from this reaction mixture which is used for optical measurements. In this way, one can study nanocrystalline ZnO particles with different sizes.

2.2. Optical Measurements. The photoluminescence measurements were performed on a SPEX Fluorolog spectrofluorometer model F2002 equipped with two double-grating 0.22 m SPEX 1680 monochromators and a 450 W xenon lamp as the excitation source. The emission spectra were corrected for the spectral response of the emission monochromator and the PM tube. Absorption measurements were performed on a Perkin-Elmer Lambda 16 UV/vis spectrophotometer.

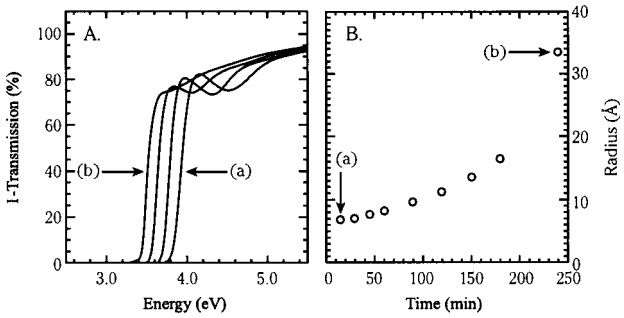

Figure 1. A: Absorption spectra of a suspension of nanocrystalline ZnO particles in 2-propanol measured at regular intervals during particle growth at room temperature. Spectrum (a) is taken after 15 min and spectrum (b) after 240 min. The two spectra between (a) and (b) are taken after 60 min and 120 min, respectively. B: Mean particle radii as determined by extrapolating the steep part of the absorption spectrum to the energy axis and using an empirical relationship between this energy value and the mean particle radius as obtained by Haase et al.[24]

Decay time measurements were performed on a Lambda Physik LPX100 XeCl Excimer laser setup (excitation with 308 nm, corresponding to 4.03 eV, with a pulse width of about 10 ns) equipped with a Jobin Yvon HR1000M monochromator and a Tektronix 2440 digital oscilloscope for the lifetime measurements.

Measurements at low temperatures were performed in the following way. A small quartz cuvette was filled with a few ml of a ZnO suspension. This cuvette was mounted on a sample holder and inserted into a flow cryostat. By flowing with liquid helium, the suspension could be cooled to 4 K. The solvent, whether it is ethanol or 2-propanol, freezes into a transparent solid.

For the decay time measurements and the low-temperature measurements, only suspensions of nanocrystalline ZnO particles in ethanol were used because of their high luminescence intensity.

3. Results

3.1. Absorption. Absorption spectra were taken at regular intervals during the growth of ZnO particles in 2-propanol at room temperature. Four of these spectra can be seen in Figure 1A. Two effects are clearly visible from these spectra. First, the absorption onset shifts to lower energies upon particle growth. Second, at the early stages of particle growth, the absorption spectra exhibit a distinct maximum directly after the onset of absorption. This feature becomes less pronounced as the aging process progresses. Both effects can be understood in terms of a decrease in quantum confinement upon particle growth. As the particle size increases, the band gap gradually shifts toward the value for macrocrystalline ZnO (~3.2 eV), hence the shift in absorption onset. Also, the density of states at the edges of the energy bands changes which leads to a less pronounced structure in the absorption spectra. From the extrapolation of the steep part of the absorption curve one can estimate the mean particle radius by using results obtained by Haase et al.[24] In this way, one can visualize the aging process of ZnO particles by plotting the mean particle radius versus time (see Figure 1B). Figure 1B shows that within a few minutes

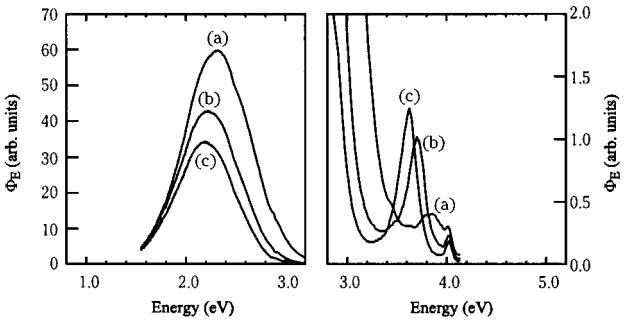

Figure 2. Emission spectra of suspensions of nanocrystalline ZnO particles in 2-propanol taken after different periods of particle growth at room temperature: (a) 15 min, (b) 120 min, and (c) 420 min. On the left, the broad visible emission band is shown and on the right the sharp UV band is visible. The ZnO particles were excited with light of 4.4 eV.

after adding the hydroxide solution to the zinc solution very small ZnO clusters are formed, with a mean radius of approximately 7 Å, corresponding to about 60 molecular ZnO units. These ZnO particles show strong quantum confinement effects. This is expected, as they are much smaller than the Bohr radius of the exciton, which is about 20 Å for macrocrystalline ZnO.

3.2. Steady-State Luminescence. Figure 2 contains three emission spectra, taken at regular intervals during the growth of ZnO particles in 2-propanol at room temperature. Each spectrum contains a weak solvent Raman peak at 4 eV, shifted with respect to the excitation energy by about 0.4 eV (3500 cm^{-1}, corresponding to an OH vibration). The relatively narrow emission band in the UV (∼3.5−3.8 eV) is due to the direct recombination of photogenerated charge carriers (exciton emission). A more intense broad emission band is observed in the visible part of the spectrum (∼2.1−2.3 eV). As can be seen from Figure 2, the UV emission band as well as the visible emission band shift to lower energies upon particle growth. The width of the exciton emission line is mainly due to inhomogeneous broadening due to a variation in particle size. For the aged particles a size distribution of about 30% has been estimated from the width of the exciton emission line and TEM pictures.[23] The line width of the broad visible emission band is mainly determined by homogeneous broadening. Electron−hole recombination at a defect site results in a large reorganization in the local charge distribution and due to this this equilibrium bond lengths change. This leads to strong vibronic transitions and broad emission bands. Still, the maximum of the broad visible emission band depends on the excitation wavelength, indicating a contribution of inhomogeneous broadening.

A second feature is evident from Figure 2. As the ZnO particles grow bigger, the intensity of the UV emission increases while that of the visible emission decreases. Figure 3 shows the intensities of both emission bands as a function of particle size. From Figure 1 it is clear that the absorbance of the samples at the excitation energy (4.4 eV) does not change much. The intensity of the visible emission decreases to about half of its original value, while that of the UV emission increases by 60%. As the intensity of the UV emission band is only a fraction of that of the visible emission band, the total integrated emission intensity decreases upon particle growth. It is well known that the visible emission band is quenched upon UV illumination in the absence of adsorbed oxygen on the surface of ZnO particles.[18] We have studied the emission of nanocrystalline ZnO particles in the presence and absence of adsorbed oxygen, on which we will report in a future publication. The size- and

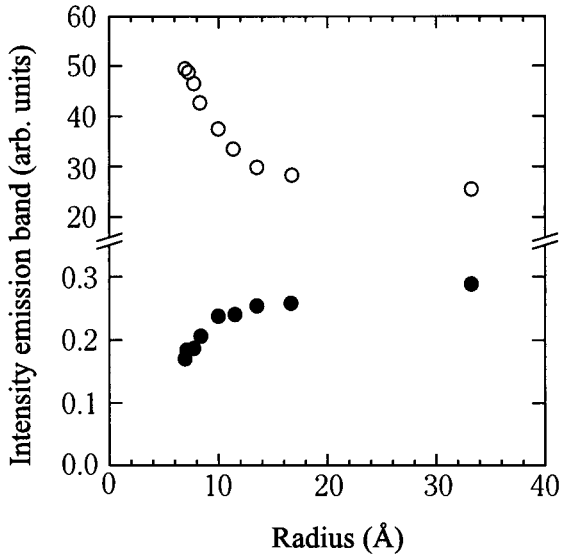

Figure 3. Dependence of the emission intensities on the particle radius for the two types of emission from nanocrystalline ZnO particles at room temperature. The solid circles represent the UV emission band and the open circles the visible emission band.

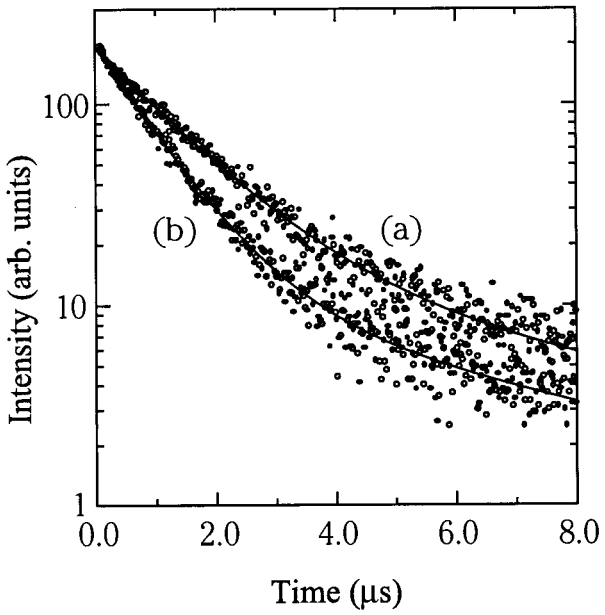

Figure 4. Luminescence lifetime measurements for the visible emission from two suspensions of nanocrystalline ZnO particles in ethanol, measured at room temperature. Curve (a) suspension of particles that are fully grown, and curve (b) suspension at an early stage of particle growth. The excitation is at 4 eV (308 nm).

temperature-dependent effects as described in this paper do not result from the absence of adsorbed oxygen as all measurements were performed in the presence of oxygen. Also, variations on a time scale of seconds or minutes, which are associated with the absence of adsorbed oxygen, are not observed.

3.3. Time-Resolved Luminescence. Decay time measurements were performed on a suspension of nanocrystalline ZnO particles in ethanol. The time evolution of the emission intensity was monitored at the maximum of the visible emission band (∼2.3 eV). The measurements were performed both at an early stage of particle growth ($R \sim 10$ Å) as well as on fully grown ZnO particles ($R \sim 30$ Å). The results are plotted in Figure 4. In both cases the decay of the visible emission intensity shows a multiexponential behavior. The experimental data points were fitted to a biexponential decay function. The fastest of the two

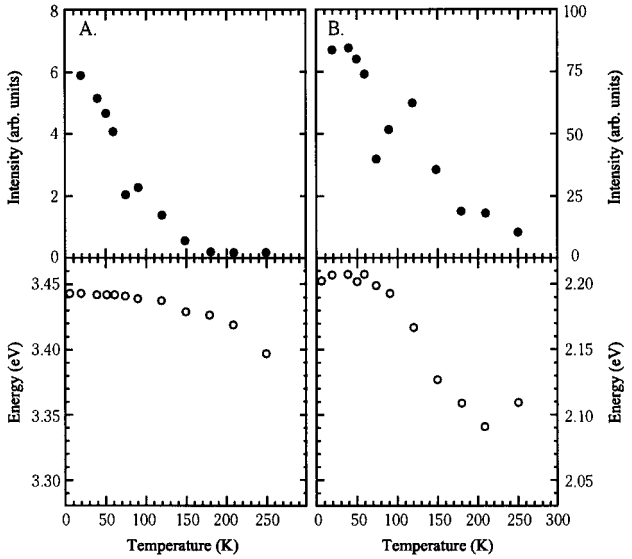

Figure 5. Temperature dependence of the emission characteristics of a suspension of nanocrystalline ZnO particles in ethanol ($R = 60$ Å). A: Ultraviolet emission. B: Visible emission. The solid circles (upper figures) represent the integrated intensities and the open circles (lower figures) the energetic positions of the maxima of the emission bands.

decay components obtained in this way made up more than 90% of the decay signal. The value of the decay time of this component is 1.34 μs for the large particles (a) and 0.92 μs for the small particles (b). This indicates that the lifetime of the visible emission increases upon particle growth. The decay time of the slower component was approximately 5 μs. For the UV emission, the lifetime was shorter than the pulse width of the laser ($\sim$10 ns) and could therefore not be measured.

3.4. Temperature-Dependent Luminescence. The emission characteristics of a suspension of nanocrystalline ZnO particles in ethanol were measured in a temperature range from 4 K to room temperature. The results of this measurement are presented in Figure 5. As the temperature increases, the intensity of both emission bands decreases. The observation that at temperatures between 70 and 120 K the intensity of the visible emission band increases is probably an artifact. Also, both emission bands shift to lower energies as the temperature increases. The temperature dependence of the maximum of the ultraviolet emission band closely resembles the temperature dependence of the band gap of macrocrystalline ZnO.[25] The maximum of the visible emission shows a different behavior. Up to 75 K, the energetic position of the maximum of the visible emission is independent of temperature. At temperatures between 75 and 180 K the maximum shifts toward lower energies by approximately 1 meV$\cdot$K^{-1}. At temperatures higher than 180 K, the energetic position is again more or less independent of temperature. In the same temperature range, the lifetime of the visible emission was monitored. In Figure 6, the decay curves at 4 K, 75 K and room temperature are shown. At 4 K, the decay of the visible emission is single exponential with a decay time of 275 ns. At 75 K, a second component with a decay time of about 1.5 μs appears in the decay curve of the visible emission. The appearance of this μs component coincides with the shift of the maximum of the visible emission to lower energies. As the temperature is increased above 75 K, the contribution of the μs component to the total decay signal increases while the intensity of the short lived luminescence decreases. At room temperature the decay of the visible emission is almost single exponential with a decay time of 1.34 μs, as was mentioned before. This

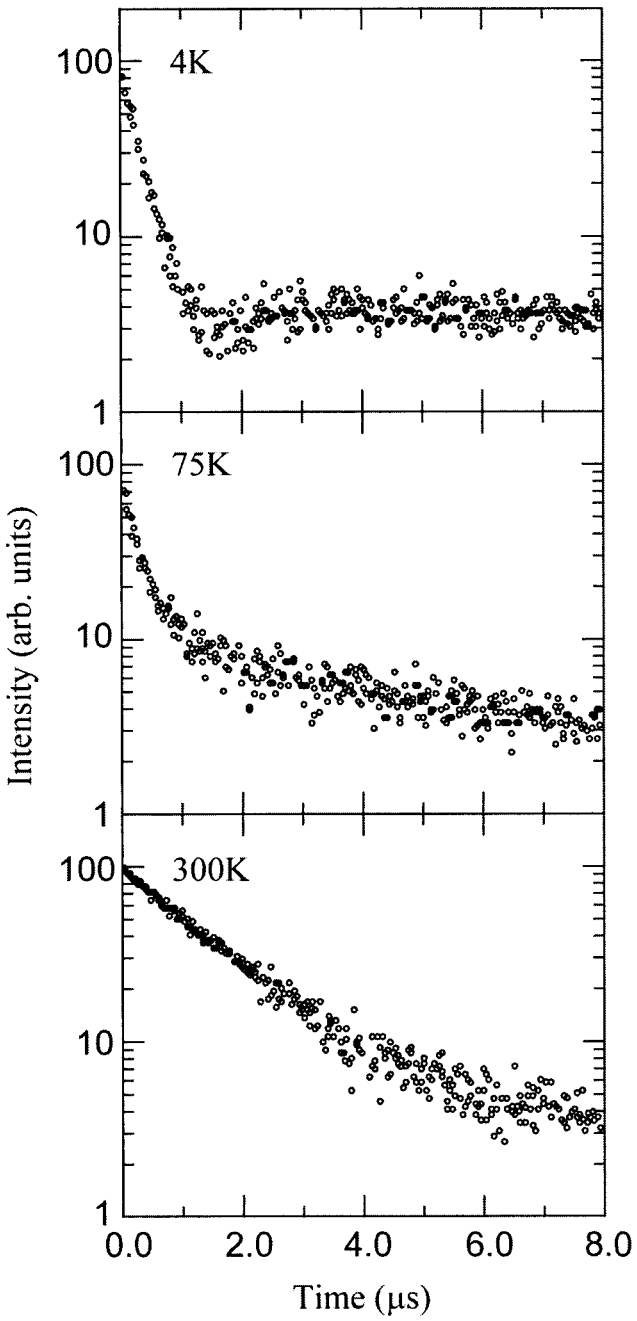

Figure 6. Luminescence decay curves of the visible emission from a suspension of nanocrystalline ZnO particles in ethanol at different temperatures. A, 4 K; B, 75 K; and C, 300 K. Excitation is at 4 eV (308 nm).

means that at low temperatures the lifetime of the visible emission is considerably shorter than at room temperature.

4. Discussion

4.1. General. Upon photoexcitation of a semiconductor particle an electron−hole pair is created. This pair can exist as a Wannier exciton and when it recombines radiatively a photon is created with an energy close to that of the band gap of the semiconductor particle. Such a process is normally referred to as exciton emission. A Wannier exciton is spatially delocalized and when the semiconductor particle is very small (i.e., in the quantum size regime) it is delocalized over the entire particle volume. The electron and/or the hole from a Wannier exciton can be trapped somewhere in the particle. This can take place

in shallow levels or in deep traps. A shallowly trapped charge carrier is still spatially delocalized. Due to this delocalization the energetic position of a shallow trap is related to the band structure of the material.[26] When the band edges shift as a function of particle size, as is the case for quantum-confined semiconductor particles, the energetic position of a shallow trap in these particles shows a similar size dependence.

When a charge carrier is trapped deeper, a localized energetic state is obtained. Such a deep trap can be found either in the bulk or at the surface of a semiconductor particle. Its energetic position is more or less independent of particle size and is determined by the chemical nature of the trap and by the local structure surrounding the trapped charge carrier. Trapping of a charge carrier can occur via a radiative process. This type of emission is referred to as trap emission. Next to these two kinds of emission (exciton and trap emission), nonradiative processes are very important in semiconductor particles. Often surface states are involved in nonradiative relaxation processes. The surface of a semiconductor is a strong perturbation of the lattice where a high concentration of both shallow and deep levels provides a pathway for nonradiative recombination of photogenerated charge carriers.[27]

4.2. Steady-State Luminescence. The size-dependent emission spectra of ZnO particles show both a visible and a UV emission band, even for the smallest particles (see Figure 2). Previously, for ZnO particles with a radius smaller than 25 Å only a visible emission was observed.[18] The energy of the maximum of the UV emission band is close to the absorption onset. This band can be assigned to the radiative recombination of Wannier excitons (exciton emission) which is a very fast process occurring on a subnanosecond time scale.

The visible emission must involve a deeply trapped charge carrier as this band is shifted by about 1.5 eV with respect to the absorption onset. Next to a deep trap level, also one of the band edges must be involved in the visible emission process because the position of this emission band depends on the particle size, as can be seen in Figure 2. By analyzing the size dependence of the emission bands, we have demonstrated in a previous paper that the visible emission is due to a transition of a photogenerated electron from a shallow level close to the conduction band edge to a deeply trapped hole (a $V_O^{\bullet\bullet}$ center[17]).

In Figure 2 it can be seen that the intensity of the visible emission band is much higher than that of the exciton emission band. However, the lifetime of the visible emission is much longer than that of the exciton emission. As both process are in competition with each other, the visible emission process must involve a step in which the photogenerated hole is trapped efficiently somewhere in the particle. The rate of this hole trapping must be much faster than the radiative recombination rate of the exciton emission. In the literature, there are indications that efficient hole trapping occurs at interfacial states in macrocrystalline ZnO.[28] Because of the large surface-to-volume ratio of our ZnO particles, efficient and fast trapping of photogenerated holes at surface sites can be expected. A good candidate for the trapping of holes are O^{2-} ions at the surface.[15] These surface ions can trap holes, thereby acting as a kind of O^{2-}/O^{-} redox couple. Evidence for the involvement of surface states in the visible emission process is provided by measurements of the temperature dependence and size dependence of the emission intensity, as will be discussed later.

4.3. Time-Resolved Luminescence at Room Temperature. The lifetime of the visible emission at room temperature is 1.34 μs for the aged particles ($R \sim 30$ Å) and 0.92 μs for the smaller particles ($R \sim 10$ Å). Lifetimes of the order of μs are typically observed for broad band trap emission in semiconductors.[29,30] If the rate-determining step in the visible emission process is the transition of a shallowly trapped electron to a deeply trapped hole, the small (but significant) size-dependence of the emission lifetime can be explained by an increase in wave function overlap between the charge carriers. For macrocrystalline semiconductors it is well known that the recombination rate of trapped charge carriers is proportional to the square of the wave function overlap.[29,31] In the smaller particles the charge carriers are closer together, resulting in a larger wave function overlap, which gives a higher oscillator strength. For CdS particles with mean diameters of 22 and 38 Å, the same lifetime has been observed for the trap emission.[29] Particles of these sizes are well within the quantum confinement regime of CdS. In the limit of very small particle sizes, the wave function of a shallowly trapped charge carrier is delocalized over the entire particle volume and the overlap with the wave function of a deeply trapped charge carrier will not increase strongly when the particle becomes even smaller.

The lifetime of the exciton emission in the UV is shorter than the time resolution of the laser setup (~10 ns). This is to be expected as a subnanosecond lifetime is typically observed for exciton emission in semiconductors. The short lifetime is due to the high oscillator strength of the transition and to fast nonradiative trapping of charge carriers. The observation that at room temperature the exciton emission is only a weak band in the UV shows that the trapping rate must be much higher than the (fast) radiative decay rate.

4.4. Temperature-Dependent Luminescence. The results from the temperature-dependent emission measurements given in Figure 5 show that the intensity of both the exciton and the trap emission increases when the temperature decreases. The increase of the exciton emission is more pronounced. It is a general observation that the luminescence efficiency is higher at low temperatures. Nonradiative pathways become more probable at higher temperatures, while radiative recombination rates are usually not significantly affected by temperature. This explains the common observation of temperature quenching.

The temperature dependence of the luminescence lifetime (as illustrated in Figure 6) is peculiar: at low temperatures ($T <$ 50 K) the lifetime of the luminescence is shorter than at higher temperatures. Usually the opposite is observed: a longer lifetime at low temperatures becomes shorter at higher temperatures due to extra (nonradiative) decay paths which require thermal activation. An explanation for the observed behavior involves a temperature-dependent population of a distribution of shallow electron traps near the conduction band edge. At low temperatures, the most shallow traps from this distribution are significantly occupied by electrons. The wave function overlap of the delocalized shallowly trapped electron and the deeply trapped hole is relatively large, resulting in a short lifetime (275 ns). Above about 50 K the shallow electron traps start to be thermally depopulated. This results in a decrease of the emission intensity since the electrons can now reach the surface and recombine nonradiatively (see also below). Alternatively, the electrons may be trapped again in somewhat deeper traps and recombine with the deeply trapped holes. This results in emission at a slightly different energy than the emission observed at lower temperatures, explaining the shift to lower energies of the emission maximum between 50 and 200 K. Since the electron wave function is less delocalized in the slightly deeper electron trap, the overlap with the wave function of the deeply trapped hole is reduced, resulting in an increase of the lifetime. The thermal detrapping of the shallowly trapped

electrons occurs between 50 and 200 K and in this temperature range the trap emission shifts to lower energies. The decay curve of the emission is two-exponential in this temperature range: both the short lifetime component (recombination of the shallowly trapped electrons) and the long lifetime component are observed. The contribution of the short decay component (275 ns) decreases between 50 and 200 K, while the contribution of the long decay component ($\sim$1 μs) increases. Above 200 K only the "slow" μs decay is observed, indicating that detrapping is complete. A similar explanation has been used before to explain temperature-dependent luminescence measurements on colloidal suspensions of CdS particles.[32]

In a study of the luminescence of nanocrystalline CdS particles, temperature quenching of the CdS trap emission was also observed, where it was explained by a multiphonon relaxation process.[29] In the case of the trap emission from nanocrystalline ZnO particles, multiphonon relaxation cannot explain the temperature quenching of this emission band. The best evidence comes from the temperature-dependent lifetime measurements as discussed above. Furthermore, the energy gap of 2 eV is too high compared to the energy of optical phonons in ZnO (0.05−0.07 eV[16]).

4.5. Nature of the Deep Hole Trap. Now that the luminescence properties of nanocrystalline ZnO particles have been discussed as a function of particle size and temperature, a more quantitative model is proposed. The nature of the deep trap involved in the visible emission is still an important issue, as discussed in the Introduction. In a previous publication we have shown that the visible emission is due to recombination of a shallowly trapped electron with a deeply trapped hole.[17] To be more specific about the nature of the deep trap, the defect chemistry of ZnO is considered. ZnO can have several types of defects such as interstitial atoms or vacancies, both anionic and cationic.[33] EPR studies have shown that oxygen vacancies containing one electron ($V_O^{\bullet}$) are the predominant paramagnetic defects.[11−13] In macrocrystalline ZnO these defects are represented by a level approximately 2 eV below the conduction band edge[33] and they are often assumed to be the recombination centers for the visible emission in ZnO. In some publications the visible emission is represented as the recombination of an electron from the conduction band with the $V_O^{\bullet}$ center (which has an effective monovalent positive charge with respect to the regular O^{2-} site).[30] After this recombination the effectively neutral $V_O^{\times}$ center is formed. The $V_O^{\times}$ center has an energy very close to the conduction band edge, and at room temperature almost all $V_O^{\times}$ centers are thermally dissociated into $V_O^{\bullet}$ centers and conduction band electrons. The shift from 2 eV below the conduction band edge for $V_O^{\bullet}$ to just below the conduction band edge for $V_O^{\times}$ is due to the correlation energy of the two electrons in the oxygen vacancy.[33] A transition of an electron from the conduction band to a $V_O^{\bullet}$ level can therefore not yield photons with an energy of 2 eV, as such a transition effectively takes place between the conduction band edge and the $V_O^{\times}$ level. This means that a mechanism in which $V_O^{\bullet}$ is the recombination center for the visible emission of ZnO is not correct. Recombination of a conduction band electron with a $V_O^{\bullet\bullet}$ center (an oxygen vacancy containing no electrons, having an effective divalent positive charge with respect to the normal O^{2-} site) can yield photons with an energy of about 2 eV. Such $V_O^{\bullet\bullet}$ centers can be formed when a hole is trapped at a $V_O^{\bullet}$ center. In the model presented below the visible emission is assigned to the recombination of a shallowly trapped electron with a deeply trapped hole in a $V_O^{\bullet\bullet}$ center.

4.6. Model. The dependence of the luminescence intensities on temperature and particle size indicates that the particle surface plays a role in the process leading to the visible emission. In view of the large surface area of the particles this is to be expected. In the preceding text it has been argued that the visible emission results from a transition that takes place in the bulk of the ZnO particle and that the recombination center is a $V_O^{\bullet\bullet}$ defect which traps an electron from a level close to the conduction band edge. In Figure 7, a schematic overview is presented of the relaxation processes of a photoexcited ZnO particle. In this figure, the band edges are shown as well as a deep trap level ($V_O^{\bullet}/V_O^{\bullet\bullet}$) and the energy distribution of a O^{2-}/O^{-} surface system. For reasons of simplicity, the shallow trapping of a photogenerated electron is not shown. A transition is indicated with an arrow and represented by the letter *T*, having a subscript that specifies the transition. This subscript consists of the initial and final state of the electron. These states are C (conduction band), V (valence band), S (surface), and T (deep trap). Nonradiative recombination is denoted with the subscript NR. In principle, this can occur at the surface (S) or at quenching centers in the particle. In view of the large surface area of the ZnO particles, only nonradiative recombination at the surface is considered.

The three competing processes on the excitonic level, shown in Figure 7A−C, are: radiative recombination with transition rate T_{CV}, trapping of the hole at the surface with rate T_{SV} (while the electron remains in the conduction band), and trapping of the electron at the surface T_{CS} (while the hole remains in the valence band). The probabilities (*P*) for these three processes are:

$$P_{CV} = \frac{T_{CV}}{T_{CV} + T_{SV} + T_{CS}} \tag{1a}$$

$$P_{SV} = \frac{T_{SV}}{T_{CV} + T_{SV} + T_{CS}} \tag{1b}$$

$$P_{CS} = \frac{T_{CS}}{T_{CV} + T_{SV} + T_{CS}} \tag{1c}$$

From absorption measurements (see Figure 1) it is clear that for ZnO particles with radii between about 10 and 30 Å, the exciton transition does not show a strong dependence on particle size. This indicates that the transition rate of the exciton recombination (T_{CV}) will not be influenced strongly by the particle size. The rates for both surface trapping processes (T_{SV} and T_{CS}) are dependent on particle size: they decrease as the particle size increases since the surface-to-bulk ratio decreases. As a result, the intensity of the exciton emission will increase with increasing particle size, as is shown in Figure 2.

On the right of Figure 7A−C, the possible consecutive relaxation steps are shown. The transition T_{CV} returns the ZnO particle to its ground state so it has no consecutive step. Trapping of the hole at the surface (Figure 7B) can have either of two possible consecutive steps. One possibility is that the surface-trapped hole tunnels back into the particle to recombine with an electron in a deep trap (T_{TS}, shown in Figure 7D). Since trap emission is observed down to the lowest temperatures it can be assumed that tunneling and not a thermally activated transfer process is operative. The other possibility is that a photogenerated electron, which is still in the conduction band, gets trapped at the surface and recombines with the surface-trapped hole (T'_{CS}, Figure 7E, the accent is used to indicate that this process is not identical to T_{CS} shown in Figure 7C). While

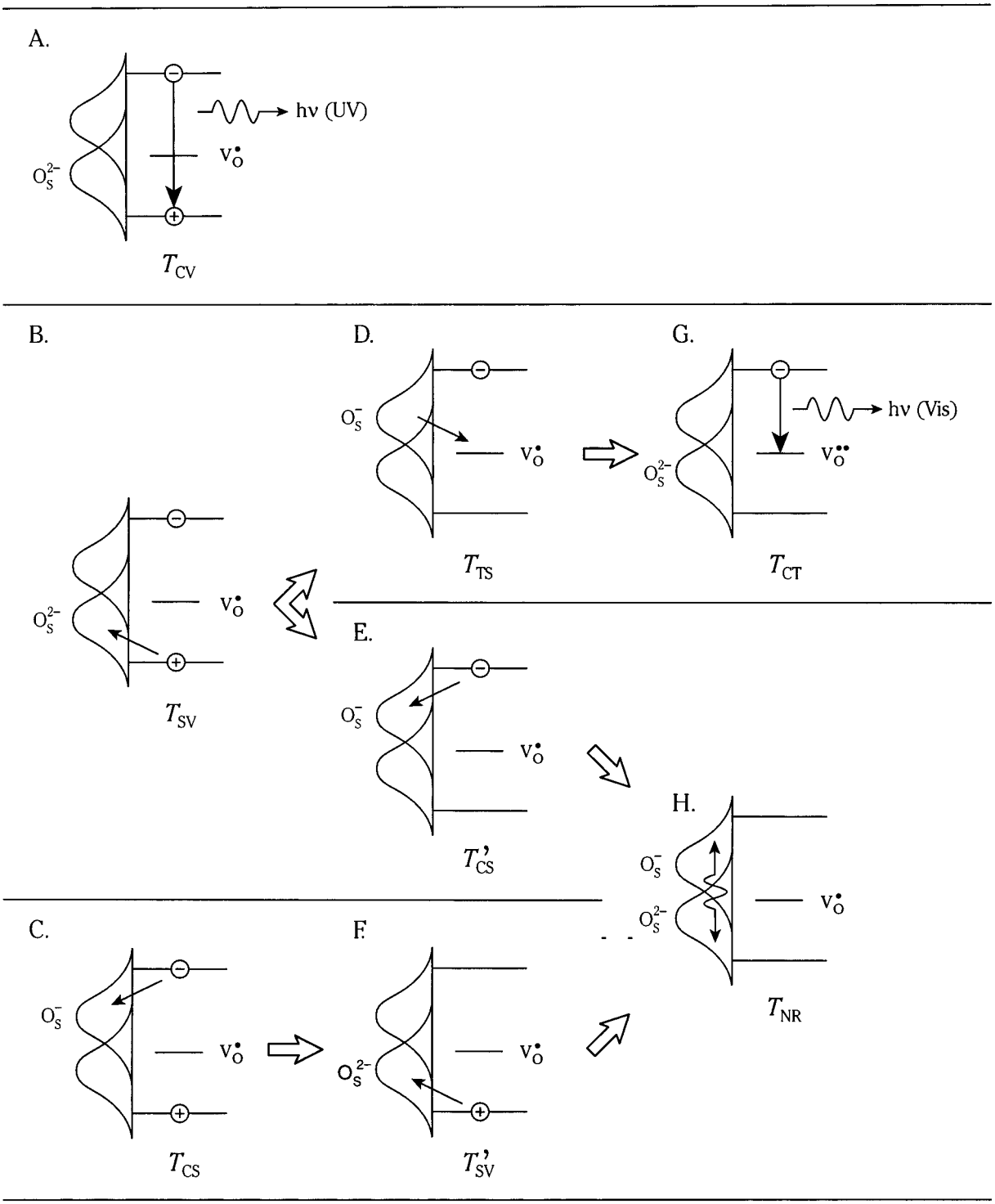

Figure 7. A schematic overview of the relaxation processes that take place upon photoexcitation of a ZnO particle. The band edges are shown as well as a deep trap level in the bulk of the particle. At the surface of the particle, an energy distribution of a O^{2-}/O^{-} system is shown. The arrows indicate a transition that is represented by the letter *T*. The subscript to this letter specifies the transition in a way that it contains the initial and final state of the electron. These states can be the conduction band (C), the valence band (V), the trap (T), or the surface (S). It is assumed that nonradiative recombination (NR) occurs only at the particle surface. A−C: Three competing processes on the level of the exciton, exciton emission and trapping of either of the charge carriers at the surface. D−E: Possible processes following surface trapping of a hole. G: Visible emission, following the tunneling of the surface-trapped hole back into the particle. H: Nonradiative recombination, which can be the result of either of two different processes, trapping of a hole at the surface followed by trapping of an electron at the surface (B and E) or trapping of an electron at the surface followed by trapping of a hole at the surface (C and F).

the former step (Figure 7D) leads to the transition responsible for the visible emission (T_{CT}, Figure 7G), the latter (Figure 7E) results in nonradiative recombination (T_{NR}, Figure 7H). When the first step in the relaxation process is the surface-trapping of an electron (Figure 7C), this will always result in nonradiative recombination (T_{NR}, Figure 7H) via surface-trapping of a hole (T'_{SV}, Figure 7F).

The three relaxation processes that return a photoexcited ZnO particle to its ground state are radiative exciton recombination (UV emission, T_{CV}), radiative trap recombination (visible

emission, T_{CT}) and nonradiative recombination at the surface (T_{NR}). The probabilities for these three processes are given by:

$$P_{CV} = \frac{T_{CV}}{T_{CV} + T_{SV} + T_{CS}} \tag{2a}$$

$$P_{CT} = \frac{P_{SV}^{\bullet}}{T_{TS} + T_{TS} + T_{CS}} \tag{2b}$$

$$P_{NR} = P_{CS} + P_{SV}\frac{T'_{CS}}{T_{TS} + T'_{CS}} \tag{2c}$$

It can easily be seen that the sum of eqs 2a, 2b, and 2c is equal to unity.

The model as presented in this paper implies that both the tunneling rate of a surface-trapped hole to a $V_O^{\bullet}$ center (T_{TS}) as well as the trapping rate of a conduction band electron at the surface (T_{CS} and T'_{CS}) decrease with increasing particle size. The tunneling rate decreases more strongly since tunneling takes place between two localized states, while the surface trapping of the conduction band electron (leading to nonradiative relaxation) involves a delocalized state. Also, the defect concentration (including $V_O^{\bullet}$ centers) may decrease when the size of the particles increases, which has been put forward before based on studies of the size-dependence of the dissolution rate of nanocrystalline ZnO particles.[34] Both effects result in a decrease of the probability for the trap emission compared to the probability for nonradiative decay at the surface. Finally, for the bigger particles also nonradiative decay in the bulk of the particle may become important and contribute to the total loss by nonradiative processes. As a result, the intensity of the trap emission decreases with increasing particle size in agreement with the experimental results (see Figures 2 and 3).

Both the trap emission and the exciton emission show thermal quenching. The quenching of the exciton emission is more pronounced. In the case of nanocrystalline ZnO particles nonradiative relaxation predominantly takes place at the surface. Nonradiative relaxation at surface sites is generally observed, and because of the large surface-to-volume ratio of nanoparticles the surface will play an important role in the quenching of the luminescence. The quenching at the surface involves trapping of both photogenerated charge carriers at the surface. With increasing temperatures the probability for surface trapping of charge carriers increases. Similar to redox couples, surface systems such as O^{2-}/O^{-} have a certain energy distribution due to solvation effects. The width of this distribution depends on the temperature: the higher the temperature, the broader the energy distribution. The larger overlap in energy between the conduction band or valence band and the surface states at higher temperatures will lead to higher trapping rates T_{SV}/T'_{SV} and T_{CS}/T'_{CS}. The exciton emission is affected by both trapping processes and therefore the temperature quenching of this emission is more pronounced. For the quenching of the trap emission, trapping of a photogenerated electron at the surface is important. Besides the increase in overlap between the conduction band states and the surface states, thermal detrapping of a shallowly trapped electron will occur at higher temperatures and the probability that an electron is trapped at surface sites at higher temperatures increases, resulting in quenching of the trap luminescence.

The model containing the possible relaxation processes of a photoexcited nanocrystalline ZnO particles as shown in Figure 7 can explain the observations qualitatively. The identification of the visible luminescence as the recombination of a conduction band electron with a deeply trapped hole at a $V_O^{\bullet\bullet}$ center is in agreement with previous work on macrocrystalline ZnO which has provided evidence for a role of oxygen vacancies in the visible luminescence of ZnO, although in these publications $V_O^{\bullet}$ centers were incorrectly assumed to be the recombination centers. In macrocrystalline ZnO also, direct trapping of holes by $V_O^{\bullet}$ centers will occur. In nanocrystalline ZnO particles an important role of the surface can be expected. Evidence for the role of fast surface-trapping of holes in the trap emission process comes from the size-dependence of the overall emission intensities and the relative intensities of the exciton and visible emission as presented in this report. The model is supported by previous work on the luminescence of nanocrystalline ZnO particles where it was observed that ions such as Fe^{2+} (ref 18) and I^{-} (ref 30), which can accept holes that are trapped at the surface of the particle, are efficient quenchers of the visible luminescence.

5. Conclusions

Temperature-dependent steady-state and time-resolved luminescence measurements were performed on suspensions of nanocrystalline ZnO particles of different sizes. All of the suspensions show two emission bands, a relatively weak and sharp UV band which can be assigned to exciton emission and a more intense and broad emission band in the visible part of the spectrum, shifted by approximately 1.5 eV with respect to the absorption onset.

A model for the kinetics of the radiative and nonradiative processes in nanocrystalline ZnO particles is proposed based on the identification of the transition responsible for the visible emission as being a recombination of a shallowly trapped electron with a deeply trapped hole. From the particle size dependence and the temperature dependence of the emission properties it is concluded that the photogenerated hole is trapped at a surface system (probably O^{2-}/O^{-}). The surface-trapped hole can tunnel back into the particle where it recombines with an electron in an oxygen vacancy ($V_O^{\bullet}$) resulting in the creation of a $V_O^{\bullet\bullet}$ center, the recombination centers for the visible emission. The dependence on particle size of the probability for this tunneling process is much stronger than that of the nonradiative processes. This results in an increase of the visible emission intensity as the size of the ZnO particles decreases.

Acknowledgment. The investigations were supported by the Council for Chemical Sciences (CW) with financial aid from The Netherlands Organization for Scientific Research (NWO).

References and Notes

(1) Shrader, R. E.; Leverenz, H. W. *J. Opt. Soc. Am.* **1947**, *37*, 939.
(2) Shionoya, S., Yen, W. M., Eds., *Phosphor Handbook*; CRC Press LCC: Boca Raton 1999; p 255.
(3) Shibahara, K.; Kuroda, N.; Nishino, S.; Matsunami, H. *Jpn. J. Appl. Phys.* **1987**, *26*, L1815.
(4) Travnikov, V. V.; Freiberg, A.; Savikhin, S. F. *J. Lumin.* **1990**, *47*, 107.
(5) Dingle, R. *Phys. Rev. Lett.* **1969**, *23* (11), 579.
(6) Mollwo, E. *Z. Phys.* **1954**, *138*, 478.
(7) Kröger, F. A.; Vink, H. J. *J. Chem. Phys.* **1954**, *22* (2), 250.
(8) Smith, J. M.; Vense, W. E. *Phys. Rev. A* **1970**, *31* (3) 147.
(9) van Craeynest, F.; Maenhout-van der Vorst, W.; Dekeyser, W. *Phys. Status Solidi* **1965**, *8*, 841.
(10) Lehman, W. *J. Electrochem. Soc.* **1968**, *115*, 538.
(11) Anpo, M.; Kubokawa, Y. *J. Phys. Chem.* **1984**, *88*, 5556.
(12) Vanheusden, K.; Seager, C. H.; Warren, W. L.; Tallant, D. R.; Voigt, J. A. *Appl. Phys. Lett.* **1996**, *68* (3), 403.
(13) Vanheusden, K.; Warren, W. L.; Seager, C. H.; Tallant, D. R.; Voigt, J. A.; Gnade, B. E. *J. Appl. Phys.* **1996**, *79* (1), 7983.
(14) Pfanel, A. *J. Electrochem. Soc.* **1962**, *109*, 502.

(15) Schoenmakers, G. H.; Vanmaekelbergh, D.; Kelly, J. J. *J. Phys. Chem.* **1996**, *100*, 3215.
(16) Madelung, O., Ed., *Landolt-Börnstein, Numerical data and functional relationships in science and technology. Volume III-17: Semiconductors*; Springer-Verlag: Berlin, 1988; 17b, pp 35−115.
(17) van Dijken, A.; Meulenkamp, E. A.; Vanmaekelbergh, D.; Meijerink, A. *J. Lumin*., accepted for publication.
(18) Bahnemann, D. W.; Kormann, C.; Hoffmann, M. R. *J. Phys. Chem.* **1987**, *91*, 3789.
(19) Koch, U.; Fojtik, A.; Weller, H.; Henglein, A. *Chem. Phys. Lett.* **1985**, *122* (5), 507.
(20) Spanhel, L.; Anderson, M. A. *J. Am. Chem. Soc*. **1991**, *113*, 2826.
(21) Meulenkamp, E. A. *J. Phys. Chem. B* **1998**, *102* (29), 5566.
(22) Wong, E. M.; Bonevich, J. E.; Searson, P. C. *J. Phys. Chem. B* **1998**, *102*, 7770.
(23) van Dijken, A.; Jansen, A. H.; Smitsmans, M. H. P.; Vanmaekelbergh, D.; Meijerink, A. *Chem. Mater*. **1998**, *10* (11), 3513.
(24) M. Haase, H. Weller, A. Henglein, *J. Phys. Chem.* **1988**, *92*, 482.
(25) Edstrup Jensen, G. H. *Phys. Status Solidi B* **1974**, *64*, K51.
(26) Brus, L. *J. Phys. Chem.* **1986**, *90*, 2555.
(27) Pankove, J. I. *Optical Processes in Semiconductors*; Dover Publications: New York, 1971.
(28) Morrison, S. R. *Electrochemistry at Semiconductor and Oxidized Metal Electrodes*, Plenum Press: New York 1980; p 227−233.
(29) Chestnoy, N.; Harris, T. D.; Hull, R.; Brus, L. E. *J. Phys. Chem.* **1986**, *90*, 3393.
(30) Kamat, P. V.; Patrick, B. *J. Phys. Chem.* **1992**, *96*, 6829.
(31) Henderson, B.; Imbusch, G. F. *Optical Spectroscopy of Inorganic Solids*, Clarendon Press: Oxford, 1989.
(32) Eychmüller, A.; Hässelbarth, A.; Katsikas, L.; Weller, H. *Ber. Bunsen-Ges. Phys. Chem.* **1991**, *95*, 79.
(33) Kröger, F. A. *The Chemistry of Imperfect Crystals*, North-Holland Publishing Company: Amsterdam 1964; p 691.
(34) Meulenkamp, E. A. *J. Phys. Chem. B* **1998**, *102*, 7764.